Ultrahigh Casimir interaction torque in nanowire systems

Tiago A. Morgado, Stanislav I. Maslovski, and Mário G. Silveirinha*

University of Coimbra, Department of Electrical Engineering–Instituto de Telecomunicações, 3030-290 Coimbra, Portugal

*mario.silveirinha@co.it.pt

Abstract: We study the Casimir torque arising from the quantum electromagnetic fluctuations due to the interaction of two interfaces in a system formed by a dense array of metallic nanorods embedded in dielectric fluids. It is demonstrated that as a consequence of the ultrahigh density of photonic states in the nanowire array it is possible to channel the quantum fluctuations, and thereby boost the Casimir torque by several orders of magnitude as compared to other known systems (e.g., birefringent parallel plates).

OCIS codes: (270.5580) Quantum electrodynamics; (160.3918) Metamaterials.

References and links

1. H. B. G. Casimir, "On the attraction between two perfectly conducting plates," Proc. K. Ned. Akad. Wet. **51**, 793–795 (1948).
2. E. M. Lifshitz, "The theory of molecular attractive force between solids," Sov. Phys. JETP **2**, 73–83 (1956).
3. I. E. Dzyaloshinskii, E. M. Lifshitz, and L. P. Pitaevskii, "The general theory of van der Waals forces," Adv. Phys. **10**(38), 165–209 (1965).
4. F. M. Serry, D. Walliser, and G. J. Maclay, "The role of the casimir effect in the static deflection and stiction of membrane strips in microelectromechanical systems MEMS," J. Appl. Phys. **84**(5), 2501–2506 (1998).
5. E. Buks and M. L. Roukes, "Stiction, adhesion energy, and the Casimir effect in micromechanical systems," Phys. Rev. B **63**(3), 033402 (2001).
6. R. Esquivel-Sirvent, L. Reyes, and J. Bárcenas, "Stability and the proximity theorem in Casimir actuated nano devices," New J. Phys. **8**(10), 241 (2006).
7. F. Capasso, J. N. Munday, D. Iannuzzi, and H. B. Chan, "Casimir forces and quantum electrodynamical torques: physics and nanomechanics," IEEE J. Sel. Top. Quantum Electron. **13**(2), 400–414 (2007).
8. H. B. Chan, V. A. Aksyuk, R. N. Kleiman, D. J. Bishop, and F. Capasso, "Quantum mechanical actuation of microelectromechanical systems by the Casimir force," Science **291**(5510), 1941–1944 (2001).
9. H. B. Chan, V. A. Aksyuk, R. N. Kleiman, D. J. Bishop, and F. Capasso, "Nonlinear micromechanical Casimir oscillator," Phys. Rev. Lett. **87**(21), 211801 (2001).
10. A. Ashourvan, M. Miri, and R. Golestanian, "Noncontact Rack and Pinion Powered by the Lateral Casimir Force," Phys. Rev. Lett. **98**(14), 140801 (2007).
11. T. Emig, "Casimir-Force-Driven Ratchets," Phys. Rev. Lett. **98**(16), 160801 (2007).
12. V. A. Parsegian and G. H. Weiss, "Dielectric anisotropy and the van der Waals interaction between bulk media," J. Adhes. **3**(4), 259–267 (1972).
13. Y. S. Barash, "Moment of van der Waals forces between anisotropic bodies," Izv. Vyss. Ucebn. Zaved. Radiofiz. **12**, 1637–1643 (1978) (Radiophys. Quantum Electron. **21**, 1138–1143 (1978)).
14. J. N. Munday, D. Iannuzzi, Y. Barash, and F. Capasso, "Torque on birefringent plates induced by quantum fluctuations," Phys. Rev. A **71**(4), 042102 (2005).
15. T. G. Philbin and U. Leonhardt, "Alternative calculation of the Casimir forces between birefringent plates," Phys. Rev. A **78**(4), 042107 (2008).
16. J. N. Munday, D. Iannuzzi, and F. Capasso, "Quantum electrodynamical torques in the presence of Brownian motion," New J. Phys. **8**(10), 244 (2006).
17. R. B. Rodrigues, P. A. M. Neto, A. Lambrecht, and S. Reynaud, "Casimir torque between corrugated metallic plates," J. Phys. A. **41**(16), 164019 (2008).
18. U. Leonhardt and T. G. Philbin, "Quantum levitation by left-handed metamaterials," New J. Phys. **9**(8), 254 (2007).
19. F. S. Rosa, D. A. Dalvit, and P. W. Milonni, "Casimir-Lifshitz Theory and Metamaterials," Phys. Rev. Lett. **100**(18), 183602 (2008).
20. R. Zhao, J. Zhou, T. Koschny, E. N. Economou, and C. M. Soukoulis, "Repulsive Casimir Force in Chiral Metamaterials," Phys. Rev. Lett. **103**(10), 103602 (2009).
21. V. Yannopapas and N. V. Vitanov, "First-Principles Study of Casimir Repulsion in Metamaterials," Phys. Rev. Lett. **103**(12), 120401 (2009).

#185968 - $15.00 USD Received 27 Feb 2013; revised 17 Apr 2013; accepted 17 Apr 2013; published 17 Jun 2013

22. M. G. Silveirinha, "Casimir interaction between metal-dielectric metamaterial slabs: Attraction at all macroscopic distances," Phys. Rev. B **82**(8), 085101 (2010).
23. M. G. Silveirinha and S. I. Maslovski, "Physical restrictions on the Casimir interaction of metal-dielectric metamaterials: An effective-medium approach," Phys. Rev. A **82**(5), 052508 (2010).
24. S. I. Maslovski and M. G. Silveirinha, "Ultralong-range Casimir-Lifshitz forces mediated by nanowire materials," Phys. Rev. A **82**(2), 022511 (2010).
25. S. I. Maslovski and M. G. Silveirinha, "Mimicking Boyer's Casimir repulsion with a nanowire material," Phys. Rev. A **83**(2), 022508 (2011).
26. M. G. Silveirinha, "Nonlocal homogenization model for a periodic array of ε-negative rods," Phys. Rev. E Stat. Nonlin. Soft Matter Phys. **73**(4), 046612 (2006).
27. P. A. Belov, R. Marques, S. I. Maslovski, I. S. Nefedov, M. Silveirinha, C. R. Simovski, and S. A. Tretyakov, "Strong spatial dispersion in wire media in the very large wavelength limit," Phys. Rev. B **67**(11), 113103 (2003).
28. M. G. Silveirinha, C. A. Fernandes, and J. R. Costa, "Additional boundary condition for a wire medium connected to a metallic surface," New J. Phys. **10**(5), 053011 (2008).
29. T. A. Morgado and M. G. Silveirinha, "Transport of an arbitrary near-field component with an array of tilted wires," New J. Phys. **11**(8), 083023 (2009).
30. N. G. Van Kampen, B. Nijboer, and K. Schram, "On the macroscopic theory of Van der Waals forces," Phys. Lett. A **26**(7), 307–308 (1968).
31. A. Lambrecht and V. N. Marachevsky, "New geometries in the Casimir effect: Dielectric gratings," J. Phys. Conf. Ser. **161**(1), 012014 (2009).
32. M. A. Ordal, R. J. Bell, R. W. Alexander, Jr., L. L. Long, and M. R. Querry, "Optical properties of fourteen metals in the infrared and far infrared: Al, Co, Cu, Au, Fe, Pb, Mo, Ni, Pd, Pt, Ag, Ti, V, and W," Appl. Opt. **24**(24), 4493–4499 (1985).

1. Introduction

In the last few years, the Casimir effect [1–3] has received considerable attention, mainly because of its importance in micro- and nano-electromechanical systems (MEMS and NEMS) [4–7]. The Casimir interactions result from the confinement of the quantum-mechanical zero-point fluctuations of the electromagnetic fields and may cause the permanent adhesion of nearby surface elements in MEMS/NEMS (a phenomenon known as 'stiction', or static friction [4,5]), severely affecting the device reliability. On the other hand, the Casimir interaction phenomena may also open new and promising directions in the field of micro and nanomechanics [8], potentially allowing for the design of, for example, Casimir oscillators [9], nanoscale racks and pinions [10], and Casimir ratchets [11].

The Casimir effect was first studied by H. Casimir in 1948. In his pioneering work [1], an attractive force between two electrically neutral metallic plates in a vacuum was predicted, as a result of the zero-point energy of the electromagnetic field. This theory was some years later generalized by E. Lifshitz to the case of dielectric plates [2], and subsequently extended to the case of having a third dielectric in between the plates [3]. A further generalization of the Casimir theory included the possibility of considering anisotropy in the plates, and was first investigated in the nonretarded regime (small separation distances) [12], and later extended to arbitrary distances [13]. In these works [12,13], it was also shown that in systems formed by two parallel birefringent plates (with in-plane optical anisotropy) a mechanical torque may arise that forces the rotation of the plates towards the position that minimizes the zero-point energy, corresponding to the alignment of the optical axes of the plates. This Casimir torque was further investigated in Refs [14,15], and some experiments aiming to observe and measure the torque were suggested [14–16]. The Casimir torque was also studied in a system formed by two parallel corrugated plates [17] when the corrugation directions are not aligned.

Recently, the Casimir-Lifshitz interaction was also investigated in structured materials (metamaterials) [18–23]. In particular, in [24,25] it was demonstrated that the Casimir interaction in systems comprising nanowire materials may be characterized by ultralong-range forces, in contrast to the short-range forces inherent to systems with isotropic backgrounds. Nanowire materials support quasi-transverse electromagnetic (q-TEM) photonic states, whose dispersion contours are hyperbolic [26]. The enhanced Casimir forces in nanowire media are a consequence of the ultra-large density of photonic states in such materials in the low frequency limit, which promotes the quantum induced interactions between the two plates in the Casimir problem, resulting in an ultralong-range force. In this work we further study the Casimir interaction in nanowire material environments, proving

#185968 - $15.00 USD Received 27 Feb 2013; revised 17 Apr 2013; accepted 17 Apr 2013; published 17 Jun 2013

that the Casimir torque in this kind of systems is qualitatively and quantitatively very different from the usual torques in either birefringent parallel plates [14,15] or corrugated metallic parallel plates [17].

2. Zero-point energy in nanowire materials

The geometry of the structure under study is illustrated in Fig. 1. It consists of a dense array of parallel metallic nanowires arranged in a square lattice with period a. The nanowires have radius r_w and are oriented along the direction $\hat{\mathbf{u}}_\alpha = \sin\alpha\hat{\mathbf{u}}_y + \cos\alpha\hat{\mathbf{u}}_z$ (forming an angle α with the z-direction) (Fig. 1), where $\hat{\mathbf{u}}_y$ and $\hat{\mathbf{u}}_z$ are the unit vectors along the coordinate axes. The nanowires are embedded in three dielectric fluids with relative permittivities $\varepsilon_{\mathrm{h},1}$, $\varepsilon_{\mathrm{h},2}$, and $\varepsilon_{\mathrm{h},3}$, respectively.

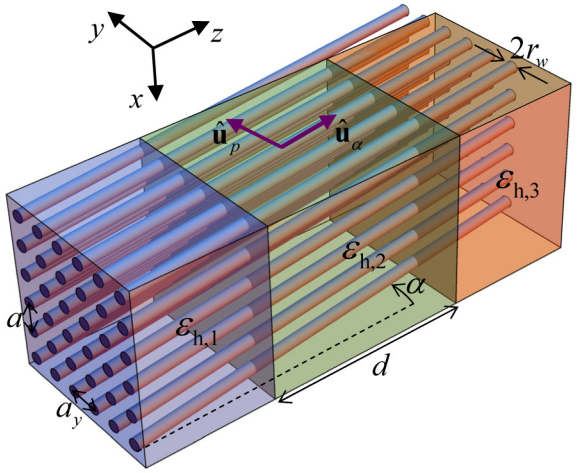

Fig. 1. Illustration of the system under study. A square array of parallel metallic nanowires embedded in three dielectric fluids. The z-axis is chosen to be orthogonal to the three dielectric layers. α is the angle between the axial direction of the nanowires ($\hat{\mathbf{u}}_\alpha$) and the z-direction.

Next, we describe the effective medium model used in this work to calculate the zero-point interaction energy of the system (Fig. 1) and discuss its validity.

2.1 Effective medium model

In general, the uniaxial wire medium is characterized by strong spatial dispersion and its electromagnetic response is described by a nonlocal dielectric function that depends on the component of the wave vector parallel to the wires $k_\alpha = \mathbf{k}\cdot\hat{\mathbf{u}}_\alpha$ ($\mathbf{k} = -i\nabla$ is the wave vector) [26–29]. Within this framework, the wire medium is modeled by the permittivity tensor $\overline{\overline{\varepsilon}}_{\mathrm{eff}} = \varepsilon_{\mathrm{h}}\left(\hat{\mathbf{u}}_x\hat{\mathbf{u}}_x + \hat{\mathbf{u}}_p\hat{\mathbf{u}}_p\right) + \varepsilon_{\alpha\alpha}\hat{\mathbf{u}}_\alpha\hat{\mathbf{u}}_\alpha$, where ε_{h} is the permittivity of the host material, and $\dfrac{\varepsilon_{\alpha\alpha}}{\varepsilon_{\mathrm{h}}} = 1 + \left[\dfrac{\varepsilon_{\mathrm{h}}}{(\varepsilon_m - \varepsilon_{\mathrm{h}})f_V} - \dfrac{\beta_{\mathrm{h}}^2 - k_\alpha^2}{\beta_p^2}\right]^{-1}$, being $\beta_{\mathrm{h}} = \omega\sqrt{\varepsilon_{\mathrm{h}}\mu_0}$ the wave number in the dielectric host, $f_V = \pi r_w^2/a^2$ is the volume fraction of the metal, a is the lattice constant, ε_m is the complex permittivity of the metallic wires, and β_p is a structural parameter with the physical meaning of plasma wave number such that $(\beta_p a)^2 \approx 2\pi\left[0.5275 + \ln\left(\dfrac{a}{2\pi r_w}\right)\right]^{-1}$. In this

#185968 - $15.00 USD Received 27 Feb 2013; revised 17 Apr 2013; accepted 17 Apr 2013; published 17 Jun 2013

work, we are interested in the case where the metallic wires are densely packed (limit $a/L_w \to 0$ with r_w/a fixed, being a the lattice constant and L_w the length of the wires), such that the relevant physics in the Casimir problem is determined by the frequency range $|\beta_h|/\beta_p << 1$, i.e. by frequencies much smaller than the effective plasma frequency of the composite medium. In such a scenario, $\varepsilon_{\alpha\alpha}$ reduces to the simple formula

$$\varepsilon_{\alpha\alpha} = \varepsilon_m f_V + (1-f_V)\varepsilon_h, \tag{1}$$

and the effective electromagnetic response is local [28,29], such that the wave propagation in the uniaxial wire medium can be described solely in terms of a transverse electric (TE) mode (ordinary wave) and of a q-TEM mode (extraordinary wave). Note that for noble metals $\varepsilon_{\alpha\alpha}$ is approximately real (in case of low loss) and negative, because ε_m has the same property. Hence, since the transverse permittivity (along directions perpendicular to the wires direction) is $\varepsilon_t = \varepsilon_h > 0$, the uniaxial wire medium behaves as an hyperbolic medium.

It can be proven (e.g. using the argument principle [22,30,31]) that, at zero absolute temperature, the regular part of the zero-point interaction energy per unity of the cross-sectional area of the system under study (Fig. 1) can be written as

$$\frac{\delta\varepsilon_C}{L_x L_y} = \frac{\hbar}{4\pi^3}\int_0^{\pi/a}\int_{-\pi/a_y}^{\pi/a_y}\int_0^{+\infty} \log D(i\xi,k_x,k_y,\alpha,d)\, d\xi dk_y dk_x, \tag{2}$$

where $\hbar = h/(2\pi)$, h is the Planck constant, ξ is the imaginary frequency ($\omega = i\xi$), $a_y = a\sec\alpha$, and $D(i\xi,k_x,k_y,\alpha,d)$ is a function such that $D=0$ represents the characteristic equation of the photonic modes supported by the pertinent cavity. Note that in the integral we only consider values of (k_x,k_y) in the semi-space $k_x > 0$, because due to symmetry the contribution from the semi-space $k_x < 0$ is equal. Moreover, to take into account the granularity of the composite material the integration region is restricted to the first Brillouin zone $\left[-\frac{\pi}{a},\frac{\pi}{a}\right]\times\left[-\frac{\pi}{a_y},\frac{\pi}{a_y}\right]$, which effectively determines a high-frequency cut-off in the wave vector space [22].

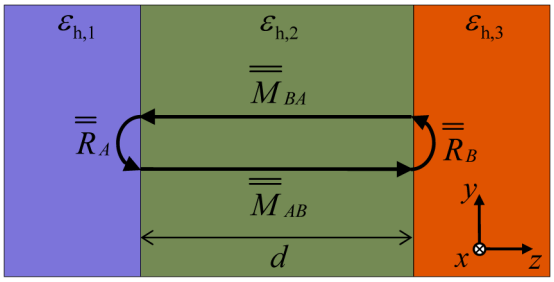

Fig. 2. A sandwich of three layers of nonmagnetic uniaxial materials with the same optical axis. The Casimir-Lifshitz energy is calculated from the reflection $\overline{\overline{R}}_{A,B}$ and transfer $\overline{\overline{M}}_{AB,BA}$ matrices.

The characteristic function $D(i\xi,k_x,k_y,\alpha,d)$ can be readily obtained as

#185968 - $15.00 USD Received 27 Feb 2013; revised 17 Apr 2013; accepted 17 Apr 2013; published 17 Jun 2013

$$D(i\xi,k_x,k_y,d,\alpha)\equiv \det[\overline{\overline{I^{(2)}}}- \overline{\overline{R}}_A(i\xi,k_x,k_y,\alpha)\cdot\overline{\overline{M}}_{AB}(i\xi,k_x,k_y,\alpha,d)\cdot\overline{\overline{R}}_B(i\xi,k_x,k_y,\alpha)\cdot\overline{\overline{M}}_{BA}(i\xi,k_x,k_y,\alpha,d)] \tag{3}$$

where $\overline{\overline{I^{(2)}}}$ is the planar unity dyadic, $\overline{\overline{R}}_{A,B}$ are the 2×2 reflection matrices of the two interfaces (see Fig. 2), and $\overline{\overline{M}}_{AB,BA}$ are the propagation matrices for the forward (waves travelling along the $+z$ direction) and backward (waves travelling along the $-z$ direction) waves, respectively, which propagate in medium 2 (see Fig. 2). The reflection matrices are defined as

$$\overline{\overline{R}}_{A,B}=\begin{pmatrix} r_{\rm co}^{\rm ord}(i\xi,k_{\|}) & r_{\rm cr}^{\rm ord}(i\xi,k_{\|}) \\ r_{\rm cr}^{\rm ext}(i\xi,k_{\|}) & r_{\rm co}^{\rm ext}(i\xi,k_{\|}) \end{pmatrix} \tag{4}$$

where $r_{\rm co}^{\rm (ord,ext)}$ is the reflection coefficient for the co-polarized wave for an incoming wave with ordinary or extraordinary polarization, respectively, and $r_{\rm cr}^{\rm (ord,ext)}$ is defined similarly but refers to the cross-polarized wave. These reflection matrices can be calculated by applying the usual boundary conditions (continuity of the tangential components of the electromagnetic fields) at both interfaces. In this calculation, the three pertinent regions of space are modeled as uniaxial dielectric media with permittivity components $\varepsilon_t=\varepsilon_{\rm h}$ and $\varepsilon_{\alpha\alpha}$, being $\varepsilon_{\alpha\alpha}$ defined as in Eq. (1) and $\varepsilon_{\rm h}=\{\varepsilon_{\rm h,1},\varepsilon_{\rm h,2},\varepsilon_{\rm h,3}\}$ depending on the region. Note that the optical axis of the effective media is tilted with the respect to the direction normal to the interfaces (*z*-direction). In this work, it is assumed that the metal is the same in the three regions, such that ε_m follows the Drude dispersion model $\varepsilon_m(i\xi)=\varepsilon_\infty+\omega_p^2/(\xi(\xi+\Gamma))$, where ε_∞ is the high-frequency permittivity, ω_p is the metal plasma oscillation frequency, and Γ is the collision frequency.

On the other hand, the propagation matrices are as follows

$$\overline{\overline{M}}_{AB,BA}=\begin{pmatrix} e^{-\gamma^{\rm ord}d} & 0 \\ 0 & e^{-\gamma_{\pm}^{\rm ext}d} \end{pmatrix}, \tag{5}$$

where the propagation constant of the ordinary wave $\gamma^{\rm ord}=-ik_z^{\rm ord}$ is given by

$$\gamma^{\rm ord}=\sqrt{\varepsilon_{\rm h,2}\mu_0\xi^2+k_x^2+k_y^2}, \tag{6}$$

and the propagation constants for the forward (wave propagating along the $+z$ direction) and backward (wave propagating along the $-z$ direction) extraordinary waves $\gamma_{\pm}^{\rm ext}$ are obtained from the dispersion characteristic

$$\frac{k_x^2+k_p^2}{\varepsilon_{\alpha\alpha}}+\frac{k_\alpha^2}{\varepsilon_{\rm h,2}}=-\xi^2\mu_0, \tag{7}$$

where $k_p=\mathbf{k}\cdot\hat{\mathbf{u}}_p$, $k_\alpha=\mathbf{k}\cdot\hat{\mathbf{u}}_\alpha$ and $\varepsilon_{\alpha\alpha}$ is defined as in Eq. (1) with $\varepsilon_{\rm h}=\varepsilon_{\rm h,2}$. In the particular case where the plasma oscillation frequency tends to infinity, $\omega_p\to\infty$, the metal behaves as a perfect electric conductor (PEC) and $\varepsilon_{\alpha\alpha}=-\infty$, so that the effective medium is characterized by "extreme anisotropy". In such a scenario, the propagation constants for the extraordinary waves are simply given by

#185968 - $15.00 USD Received 27 Feb 2013; revised 17 Apr 2013; accepted 17 Apr 2013; published 17 Jun 2013

$$\gamma_{\pm}^{\text{ext}} = \sqrt{\varepsilon_{\text{h},2}\mu_0}\,\xi \sec\alpha \pm ik_y \tan\alpha. \tag{8}$$

2.2 On the validity of the effective medium model

To assess the validity of the effective medium model in the calculation of the Casimir-Lifshitz forces – particularly the fact that spatial dispersion is neglected - next we compare the results obtained based on the hyperbolic medium approximation [Eq. (1)] with the more general theory of Ref [24] that takes into account the nonlocal dispersive behavior of the nanowire materials [26,27]. In these calculations, we only consider the case $\alpha = 0^\circ$ so that the wires are perpendicular to the interfaces.

In Ref [24], it was shown that the Casimir force in nanowire environments is an ultralong-range force that decays as $1/d^2$, which contrasts markedly with the characteristic decay of $1/d^4$ in usual systems with isotropic backgrounds. This anomalously high Casimir interaction stems from the fact that arrays of nanowires support q-TEM waves that allow channeling the quantum oscillations of the electromagnetic field, boosting in this way the intensity of the Casimir force at large distances. It was demonstrated in [24] that the contribution to the Casimir force of the other electromagnetic modes (TM and TE modes) that propagate in the wire medium may be negligible (especially for large distances), since these modes contribute only to short-range forces that decay quickly with the distance. Hence, based on Ref [24], the Casimir force (or more rigorously, the contribution of the q-TEM modes to the Casimir force) per unit of area in systems formed by arbitrary nondispersive magnetodielectrics embedded in nanowire materials is given by:

$$\frac{F_{\text{TEM}}}{L_x L_y} = \frac{\hbar c\, \text{Li}_2(r_1 r_2)}{4\pi a^2 d^2}, \tag{9}$$

where $\text{Li}_2(z) = \sum_{n=1}^{\infty} z^n / n^2$ is the polylogarithm function of order two, and $r_{1,2}$ are the reflection coefficients at the boundaries for normal incidence. In the particular case of a system comprising two PEC plates ($r_1 r_2 = 1$) with an array of metallic nanorods between them [top inset of Fig. 3], the Casimir force is simply

$$\frac{F_{\text{TEM}}}{L_x L_y} = \frac{\pi}{24}\frac{\hbar c}{a^2 d^2}. \tag{10}$$

In this work, we follow the same convention as in Refs [1,24]: a positive force corresponds to attraction, whereas a negative force corresponds to repulsion.

In Fig. 3, we compare the normalized Casimir force F_{C} as a function of the distance d calculated using the hyperbolic medium model [$F_{\text{C}} = -\partial \delta\varepsilon_{\text{C}} / \partial d$, where $\delta\varepsilon_{\text{C}}$ is the zero-point energy obtained from Eq. (2)] (discrete symbols) with the results based on the nonlocal model of Ref [24] (solid lines). There is an excellent agreement between the two theories, even when the effect of loss and dispersion in the metal nanowires is considered, supporting in this manner the validity of the simplified effective medium model in the context of the Casimir problem. Note, however, that such an agreement can be obtained only by restricting the (k_x, k_y) integration in Eq. (2) to the first Brillouin zone, which in effect takes into account the wire medium granularity and recovers the $1/d^2$ dependence of the Casimir force with distance in such systems. It is also clear that the effect of metallic loss and dispersion is quite mild, since the magnitude of the Casimir force for Ag nanowires is only slightly lower than that for PEC nanowires.

#185968 - $15.00 USD Received 27 Feb 2013; revised 17 Apr 2013; accepted 17 Apr 2013; published 17 Jun 2013

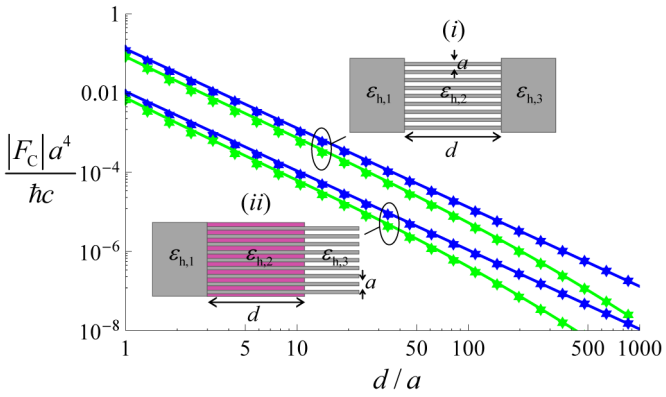

Fig. 3. Normalized Casimir forces as functions of the normalized distance for two different system configurations shown in the insets. (*i*) Configuration I: PEC – nanowires embedded in air – PEC; (*ii*) Configuration II: nanowires embedded in three nonmagnetic materials (PEC – bromobenzene – air). In both cases, $a = 100$ nm and $r_w = 20$ nm. Solid lines: Contribution of the q-TEM modes to the Casimir force calculated with the nonlocal model of Ref [24]; Discrete symbols: Casimir forces calculated using the hyperbolic medium model described in Subsection 2.1. Blue lines and symbols: PEC nanowires; Green lines and symbols: lossy and dispersive Ag nanowires modeled by a Drude-type dielectric function with parameters taken from the literature [32].

The results of Fig. 3 confirm that the contribution of the TE mode to the Casimir force is indeed residual. Indeed, in our calculation (discrete symbols of Fig. 3), both the contributions of the q-TEM modes (extraordinary wave) and TE modes (ordinary wave) are taken into account. Finally, it is important to point out that the Casimir force is attractive for the configuration I (Fig. 3(*i*)), whereas in the other scenario the Casimir force is repulsive (Fig. 3(*ii*)).

3. Casimir torque in nanowire materials

In this section, we calculate the Casimir interaction torque acting on the metallic nanowires in the system illustrated in Fig. 1 formed by two interacting interfaces separated by a distance d. One important point is that for this type of systems the Casimir torque may be nonzero even when the distance d between the two interfaces approaches infinity. Indeed, it should be clear that even for a single interface the zero-point energy stored in the system may depend on the angle α that defines the orientation of the nanowires, and therefore, one should expect a remnant Casimir torque when $d \to \infty$. This property is specific of our system, and is not found in other geometries studied hitherto [14,15,17]. For example, due to the isotropy of the vacuum the zero-point energy of a single birefringent plate standing alone in free-space is independent of its relative orientation, and thus the Casimir induced torque for a pair of birefringent plates vanishes when $d \to \infty$.

Obviously, because of the electromagnetic coupling between the two interfaces, the torque will depend on d, such that the total torque can be written as $M_C = M_{C,12} + M_{C,32} + M_{C,int}$, being $M_{C,12}$ the remnant torque associated with the first interface (between the dielectrics $\varepsilon_{h,1}$ and $\varepsilon_{h,2}$), $M_{C,23}$ the remnant torque associated with the second interface (between the dielectrics $\varepsilon_{h,2}$ and $\varepsilon_{h,3}$), and $M_{C,int}$ the interaction torque resulting from the coupling between the two interfaces. In this work, we present a detailed analysis of the calculation of the interaction torque, and derive a rough analytical estimation for the single-interface Casimir torques ($M_{C,12}$ and $M_{C,23}$).

#185968 - $15.00 USD Received 27 Feb 2013; revised 17 Apr 2013; accepted 17 Apr 2013; published 17 Jun 2013

3.1 Theoretical analysis

The Casimir torque M_{C} per unit of area can be expressed in terms of the zero-point energy of the system as [13]

$$\frac{M_{\mathrm{C}}}{L_x L_y} = -\frac{\partial}{\partial \alpha}\left(\frac{\varepsilon_{\mathrm{C}}}{L_x L_y}\right). \tag{11}$$

In typical systems, the Casimir energy ε_{C} can be simply replaced by the interaction energy $\delta\varepsilon_{\mathrm{C}}$ given by Eq. (2). However, because our background (region 2) is not isotropic, here we need to proceed carefully. Indeed, it should be noted that

$$\varepsilon_{\mathrm{C}}(d,\alpha) = \varepsilon_{\mathrm{C}}(d \to \infty,\alpha) + \delta\varepsilon_{\mathrm{C}}(d,\alpha). \tag{12}$$

The term $\varepsilon_{\mathrm{C}}(d \to \infty,\alpha)$ corresponds to the Casimir energy when the regions 1 and 3 are infinitely far apart. It does not contribute to the usual Casimir force (because it is independent of *d*) but it may contribute to the Casimir torque because it depends on α. This additional contribution to the torque is easy to understand from a physical point of view. Indeed, as discussed previously, even in the presence of a single material interface (let us say between medium 1 and medium 2) there may still exist a torque acting on the metallic wires because they are tilted with respect to the interface. Therefore, we can write:

$$\begin{aligned}\frac{M_{\mathrm{C}}}{L_x L_y} &= \frac{M_{\mathrm{C,int}}}{L_x L_y} + \frac{M_{\mathrm{C,12}}}{L_x L_y} + \frac{M_{\mathrm{C,32}}}{L_x L_y} \\ &= -\frac{\partial}{\partial \alpha}\left(\frac{\delta\varepsilon_{\mathrm{C}}}{L_x L_y}\right) - \frac{\partial}{\partial \alpha}\left(\frac{\varepsilon_{\mathrm{C,12}}}{L_x L_y}\right) - \frac{\partial}{\partial \alpha}\left(\frac{\varepsilon_{\mathrm{C,32}}}{L_x L_y}\right).\end{aligned} \tag{13}$$

being $M_{\mathrm{C,12}}$ and $M_{\mathrm{C,32}}$ the torques induced in case of single 1-2 (configuration of Fig. 4(a)) and 2-3 material interfaces, and $\varepsilon_{\mathrm{C,12}}$ and $\varepsilon_{\mathrm{C,32}}$ are the corresponding zero-point energies, which are independent of *d*.

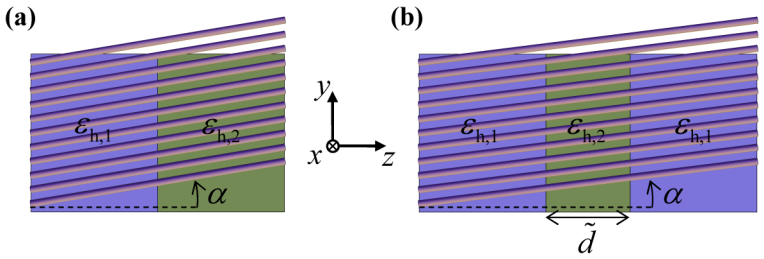

Fig. 4. Nanowire material system configurations. (a) Single-interface configuration; (b) Twin-interface configuration.

The interaction torque $\frac{M_{\mathrm{C,int}}}{L_x L_y} = -\frac{\partial}{\partial \alpha}\left(\frac{\delta\varepsilon_{\mathrm{C}}}{L_x L_y}\right)$ can be readily evaluated with the help of Eq. (2). In the next two subsections we derive an analytical estimation for $M_{\mathrm{C,int}}$ and discuss how the single-interface torques $M_{\mathrm{C,12}}$ and $M_{\mathrm{C,32}}$ can be determined.

#185968 - $15.00 USD Received 27 Feb 2013; revised 17 Apr 2013; accepted 17 Apr 2013; published 17 Jun 2013

3.2 Analytical expression for the interaction torque

To obtain a closed analytical formula for the Casimir interaction torque induced in the nanowire material (see Fig. 1), next we generalize the theory of [24] and compute the contribution of the q-TEM photonic modes to the Casimir interaction energy when the angle α is in the range $0° < \alpha < 90°$. To do this, we consider the case wherein the nanowire materials are characterized by extreme anisotropy so that $\varepsilon_{\alpha\alpha} = -\infty$ in the relevant frequency range. In such a situation the reflection coefficient for a q-TEM wave incident upon an interface of two nanowire materials (let us say, propagating from region 2 to region 1) with different dielectric hosts is nearly independent of $\mathbf{k}_{\|}$ ($\mathbf{k}_{\|} = \mathbf{k} - \mathbf{k}\cdot\hat{\mathbf{u}}_\alpha\hat{\mathbf{u}}_\alpha$), and is approximately equal to $r = \dfrac{\eta_1 - \eta_2}{\eta_1 + \eta_2}$, being $\eta = \sqrt{\mu_0/\varepsilon_h}$ the wave impedance in the pertinent dielectric host. Therefore the zero-point energy in the nanowire configuration sketched in Fig. 1 can be written as follows:

$$\frac{\delta\varepsilon_C}{L_x L_y} = \frac{\hbar}{2\pi}\int_{-\pi/a}^{\pi/a}\int_{-\pi/a_y}^{\pi/a_y}\frac{dk_y dk_x}{(2\pi)^2}\int_0^{+\infty}\log(1 - r_1 r_2 e^{-\gamma_+ d}e^{-\gamma_- d})d\xi, \tag{14}$$

where $\gamma_\pm$ are the propagation constants of the q-TEM mode [see Eq. (8)] and r_1 and r_2 are the reflection coefficients at the two interfaces. Making the change of variables $t = 2d\sqrt{\varepsilon_{h,2}\mu_0}\sec\alpha\,\xi$, the Casimir interaction energy at zero temperature becomes

$$\frac{\delta\varepsilon_C}{L_x L_y} = \frac{\hbar}{4\pi}\frac{\cos^2\alpha}{\sqrt{\mu_0\varepsilon_{h,2}}a^2 d}\int_0^{+\infty}\log(1 - r_1 r_2 e^{-t})dt = -\frac{\hbar}{4\pi}\frac{\cos^2\alpha}{\sqrt{\mu_0\varepsilon_{h,2}}a^2 d}\mathrm{Li}_2(r_1 r_2). \tag{15}$$

Notice that we can write $\dfrac{\delta\varepsilon_C}{L_x L_y}(\alpha) = \cos^2\alpha\left.\dfrac{\delta\varepsilon_C}{L_x L_y}\right|_{\alpha=0}$. Thus, the contribution to the torque due to the interaction between medium 1 and 3 is given by

$$\frac{M_{C,int}}{L_x L_y} = -\frac{\partial}{\partial\alpha}\left(\frac{\delta\varepsilon_C}{L_x L_y}\right) = \sin(2\alpha)\left.\frac{\delta\varepsilon_C}{L_x L_y}\right|_{\alpha=0}. \tag{16}$$

Interestingly, one can see that the interaction torque induced in metallic nanowires varies as $\sin(2\alpha)$, similar to the behavior of the torque in the configuration discussed in [13–15].

3.3 Single-interface torque

In order to determine $M_{C,12}$ ($M_{C,32}$ is determined in the same manner), we consider the scenario of Fig. 4(b), which represents a twin-interface configuration wherein $\varepsilon_{h,1} = \varepsilon_{h,3}$ and the distance between the two interfaces is $\tilde{d}$. The same analysis that led to Eq. (13) shows that for the scenario of Fig. 4(b) one can write:

$$\frac{\tilde{M}_{C.12}}{L_x L_y} = -\frac{\partial}{\partial\alpha}\left(\frac{\delta\tilde{\varepsilon}_{C,12}}{L_x L_y}\right) - 2\frac{\partial}{\partial\alpha}\left(\frac{\varepsilon_{C,12}}{L_x L_y}\right). \tag{17}$$

being $\tilde{M}_{C,12}$ and $\delta\tilde{\varepsilon}_{C,12}$ the torque and interaction energy for this scenario, which depend on α and $\tilde{d}$. But on physical grounds it is clear that if the gap $\tilde{d}$ is closed the torque in the scenario of Fig. 4(b) must vanish, because in such a situation the nanowires are embedded in

#185968 - $15.00 USD Received 27 Feb 2013; revised 17 Apr 2013; accepted 17 Apr 2013; published 17 Jun 2013

a uniform background. Thus, we can write $-\frac{\partial}{\partial\alpha}\left(\frac{\mathcal{E}_{\mathrm{C},12}}{L_x L_y}\right)=\lim_{\tilde{d}\to 0}\frac{1}{2}\frac{\partial}{\partial\alpha}\left(\frac{\delta\tilde{\mathcal{E}}_{\mathrm{C},12}}{L_x L_y}\right)$ or equivalently:

$$\frac{M_{\mathrm{C},12}}{L_x L_y}=\lim_{\tilde{d}\to 0}\frac{1}{2}\frac{\partial}{\partial\alpha}\left(\frac{\delta\tilde{\mathcal{E}}_{\mathrm{C},12}}{L_x L_y}\right). \tag{18}$$

Therefore, we were able to express the single-interface torque in terms of the interaction energy associated with the scenario of Fig. 4(b). Notice that the limit $\tilde{d}\to 0$ needs to be taken in the calculation. This is challenging for several reasons.

Indeed, this torque is determined by the near-field interactions (at the interface) of the metallic wires and the host materials, and thus the contribution of higher-order modes (not described by the effective medium model) is likely to be important. In the context of the Casimir problem the use of the effective medium model is accurate only when $\tilde{d}>a$.

Nevertheless, one may estimate $M_{\mathrm{C},12}$ based on the continuous medium approximation, but even in such a case things are not plain. In fact, unless one adopts a realistic dispersive model for the dielectrics and metal so that their electric response vanishes for $\omega\to\infty$, the zero-point energy $\delta\tilde{\mathcal{E}}_{\mathrm{C},12}$ typically diverges in the limit $\tilde{d}\to 0$.

Considering these limitations, next we obtain an analytical formula for $M_{\mathrm{C},12}$ based on the continuous material approximation, under the hypothesis that all the material responses cease at $\xi=\xi_{\max}$, beyond which the contribution of higher-order modes should be included and the effective medium theory breaks down. It is evident that in general this limit may depend on the wire tilting angle α. It is reasonable to assume on physical grounds that $\xi_{\max}(\alpha)\approx c\frac{\pi}{a_y}=c\frac{\pi}{a}\cos\alpha$. Proceeding as in Subsection 3.2, we find that:

$$\begin{aligned}\frac{\delta\tilde{\mathcal{E}}_{\mathrm{C},12}}{L_x L_y}&=\frac{\hbar}{2\pi}\int_{-\pi/a}^{\pi/a}\int_{-\pi/a_y}^{\pi/a_y}\frac{dk_y dk_x}{(2\pi)^2}\int_0^{\xi_{\max}}\log(1-r_1^2 e^{-\gamma_+\tilde{d}}e^{-\gamma_-\tilde{d}})d\xi\\&=\frac{\hbar}{2\pi}\frac{\cos\alpha}{a^2}\int_0^{\xi_{\max}}\log(1-r_1^2 e^{-2\tilde{d}\sqrt{\varepsilon_{\mathrm{h},2}\mu_0}\sec\alpha\,\xi})d\xi.\end{aligned} \tag{19}$$

Taking the limit $\tilde{d}\to 0$ and using Eq. (18) we obtain the desired result:

$$\frac{M_{\mathrm{C},12}}{L_x L_y}=\frac{\hbar c}{4}\frac{\sin 2\alpha}{a^3}\log\left(\frac{1}{1-r_1^2}\right). \tag{20}$$

Notice that this remnant torque vanishes for $\alpha=0^{\circ}$ (wires perpendicular to the interface) and $\alpha=90^{\circ}$ (wires parallel to the interface), being the latter situation the one corresponding to a stable equilibrium. This means that small angular deviations from $\alpha=90^{\circ}$ result in torques rotating the nanorods back to this equilibrium position, whereas slight angular variations from $\alpha=0^{\circ}$ result in torques pushing the nanorods away from this position.

It is interesting to look at the problem from a different perspective, and suppose that the nanowires are held fixed, whereas the dielectric hosts (e.g. two immiscible fluids such as water and olive oil) are free to be rotated. In this scenario, the Casimir torque induced in the system may force the dielectric fluids to move in such a manner that the interface moves toward the position of stable equilibrium where $\alpha=90^{\circ}$. Perturbations in the alignment of

#185968 - $15.00 USD Received 27 Feb 2013; revised 17 Apr 2013; accepted 17 Apr 2013; published 17 Jun 2013

the interfaces with respect to the orientation of the nanowires may provide a "signature" of the Casimir torque that may permit detecting it experimentally.

3.4 Numerical results and discussion

Next, we present a numerical study of the Casimir interaction torque ($M_{\mathrm{C,int}}$), i.e. of the perturbation of the total torque resulting from the electromagnetic coupling of the two interfaces, for several illustrative cases.

We have calculated the Casimir interaction torque $M_{\mathrm{C,int}}$ induced in the nanowire system sketched in Fig. 1 for different angles α and for a fixed distance $d = 4\ \mu$m, using both the analytical model [Eq. (16)] and the hyperbolic medium model [$M_{\mathrm{C,int}} = -\partial \delta\varepsilon_{\mathrm{C}} / \partial\alpha$, where $\delta\varepsilon_{\mathrm{C}}$ is the zero-point energy obtained from Eq. (2)]. The results are depicted in Fig. 5(*i*).

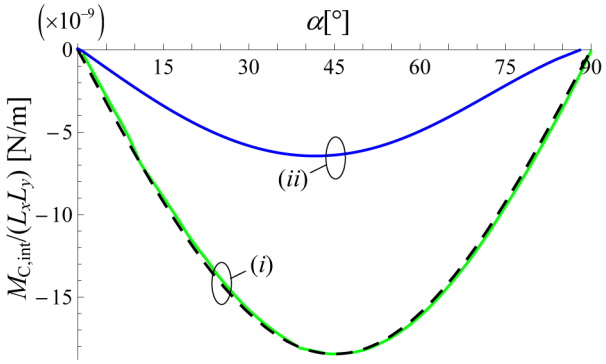

Fig. 5. Casimir interaction torque $M_{\mathrm{C,int}}$ per unity of the cross-sectional area as a function of α for a nanowire configuration as illustrated in Fig. 1 with $\varepsilon_{\mathrm{h},1} = \varepsilon_{\mathrm{h},3} = 80.4$ (water) and $\varepsilon_{\mathrm{h},2} = 3.1$ (olive oil). Solid lines: Casimir interaction torques calculated using the hyperbolic medium model described in Subsection 2.1. Dashed line: Casimir interaction torque calculated using the analytical formula derived in Subsection 3.2. (*i*) PEC nanowires; (*ii*) Ag nanowires. In all these plots $a = 100$ nm, $r_w = 17.84$ nm, and $d = 4\ \mu$m.

First, it is important to highlight the very good agreement between the results obtained with the two different calculation methods. Similar to the analytical model (black dashed curve), the numerical results (green solid curve) also predict that the Casimir interaction torque varies as $\sin(2\alpha)$. Moreover, the maximum magnitude of the Casimir interaction torque occurs at $\alpha = 45°$. On the other hand, the Casimir interaction torque is null when the nanowires are parallel ($\alpha = 90°$) or perpendicular ($\alpha = 0°$) to the interface planes, similar to the single-interface torques. For the case of twin-material interfaces ($\varepsilon_{\mathrm{h},1} = \varepsilon_{\mathrm{h},3}$) the sign of the interaction torque is opposite to that of the single-interface torques, consistent with the fact that if the gap closes the total torque $M_{\mathrm{C}} = 2M_{\mathrm{C,12}} + M_{\mathrm{C,int}}$ should vanish. Therefore, in this case, the interaction of the two interfaces leads to a depression of the Casimir torque.

The results of Fig. 5(*i*) also prove that the contribution of the TE mode to the Casimir interaction can be neglected, since the result predicted by our numerical calculation (which takes into account the contribution of the TE mode) is quantitatively very similar to the one obtained from the analytical model (which only takes into consideration the contribution of the q-TEM mode).

In the previous example, it was assumed that the nanowires are PECs. To assess the effect of metallic loss and dispersion, we have also calculated the Casimir interaction torque in the nanowire system of Fig. 1 for Ag nanorods (Fig. 5(*ii*)) [Ag is described by a Drude dispersion

#185968 - $15.00 USD Received 27 Feb 2013; revised 17 Apr 2013; accepted 17 Apr 2013; published 17 Jun 2013

model [32]]. As can be seen, the behavior of the Casimir interaction torque with the angle α for Ag nanowires is qualitatively similar to that of PEC nanowires, but the system with Ag nanowires generates a slightly weaker Casimir interaction torque.

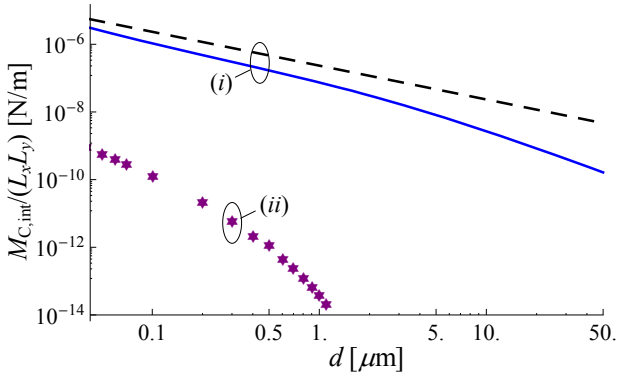

Fig. 6. Casimir interaction torque $M_{C,int}$ per unity of the cross-sectional area as a function of the distance d for $\alpha = 45^{\circ}$. (*i*) Nanowire configuration illustrated in Fig. 1 with $\varepsilon_{h,1} = \varepsilon_{h,3} = 80.4$, $\varepsilon_{h,2} = 3.1$, $a = 100$ nm, and $r_w = 17.84$ nm; Dashed line: PEC nanowires; Solid line: Ag nanowires. (*ii*) Casimir torque in a system formed by two 20 μm thick calcite and barium titanate ($BaTiO_3$) plates in vacuum as considered in Ref [14].

We have also calculated the magnitude of the Casimir interaction torque at $\alpha = 45°$ as a function of the distance d (Fig. 6). We show the results of the Casimir torque for both PEC nanowires [black dashed curve] and Ag nanowires [blue solid curve]. Again, the dependence of the Casimir interaction torque on metallic loss and dispersion is relatively weak, since the difference between the PEC and Ag nanowires results is modest.

In addition, we also show in Fig. 6 the magnitude of the Casimir torque in the system discussed in Ref [14] formed by a two parallel birefringent plates (calcite and barium titanate) separated by a vacuum. It is seen from Fig. 6 that the Casimir interaction torque induced in the nanowire configuration illustrated in Fig. 1 is several orders of magnitude larger than the torque generated in the birefringent plates system [14]. In particular, the difference between the magnitudes of the torques is increasingly pronounced as the distance d is increased. In fact, this result was expected because for the configuration of Ref [14] the Casimir torque decays approximately as $1/d^3$, whereas it was found in Subsection 3.2 that in the proposed nanowire system the Casimir interaction torque decays as $1/d$ (see Eqs. (15-16)). It is important not to forget that the total torque also depends on $M_{C,12}$ and $M_{C,23}$ which typically are nonzero in case of the nanowire system, but vanish in the system of Ref [14].

4. Conclusion

In this work, we have studied analytically and numerically the Casimir interaction torque induced in a system formed by a dense array of metallic nanowires embedded in three dielectric fluids (modeled as hyperbolic media). It was demonstrated that the perturbations in the torque resulting from the interaction of the two interfaces is several orders of magnitude larger than the torque generated in other structures reported in the literature (e.g., birefringent parallel plates, or even corrugated metallic parallel plates). In particular, it was found that in the nanowire structures the Casimir interaction torque decays as $1/d$, in contrast to the decay $1/d^3$ that characterizes the usual setups comprising two parallel plates. The reason is that nanowire hyperbolic materials have a large density of photonic modes in the low-frequency limit, which promotes the quantum induced interactions. We have also estimated a

#185968 - $15.00 USD Received 27 Feb 2013; revised 17 Apr 2013; accepted 17 Apr 2013; published 17 Jun 2013

contribution to the Casimir torque resulting from the near-field interactions of the nanowires passing through a single dielectric interface. Generally, this contribution to the torque cannot be obtained within the framework of a continuous medium model, as it depends on the microstructure of the metamaterial in the vicinity of the interface.

Acknowledgments

This work is supported in part by Fundação para Ciência e a Tecnologia under project PTDC/EEATEL/100245/2008.

#185968 - $15.00 USD Received 27 Feb 2013; revised 17 Apr 2013; accepted 17 Apr 2013; published 17 Jun 2013